Effect of UV Curing on Electrical Properties of a UV-Curable *co*-Polyacrylate/Silica Nanocomposite as a Transparent Encapsulation Resin for Device Packaging

Yu-Young Wang, Tsung-Eong Hsieh*

Electrical properties of UV-curable *co*-polyacrylate/silica nanocomposite resins prepared via sol-gel process for device encapsulation were investigated. It was found that, by appropriate UV curing process and the formation of nanoscale silica particles finely dispersed in the resin matrix, the leakage current density of the nanocomposite resin films decreases from 235 to 1.3 $nA \cdot cm^{-2}$ at the applied electrical field of 10 $kV \cdot cm^{-1}$. The silica nanoparticles also restricted the motions of polar functional groups in organic matrix that the nanocomposite films with satisfactory dielectric properties [dielectric constant (ε) = 3.93 and tangent loss ($\tan\delta$ = 0.0472) could be obtained. Chemical structure analyses revealed that excessive UV curing results in photooxidation and/or photodegradation in resin samples, leading to the polar groups and ionic/radical segments in organic matrix as well as the –Si–O–Si– structure in the vicinity of silica nanoparticles. These organic/inorganic functional groups generated more permeation paths for charge carrier migration and hence deteriorated the electrical properties of the nanocomposite samples. Though post-baking treatment at 80 °C for 1 h followed by UV curing improved the rigidity of the resin sample, it brought the polar functional groups closer to each other and similarly degraded electrical properties of the nanocomposite resins.

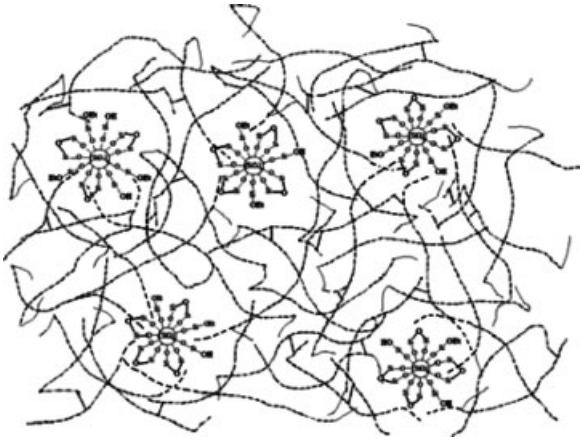

Introduction

The UV-curable adhesive resins have been widely applied to the encapsulation of optoelectronic devices.[1–3] In particular, they are the key materials for the packaging of modern flat panel displays (FPDs) such as organic light-emitting devices (OLEDs) since the sealing processes utilizing thermal-curable resins are incompatible to the light-emitting material and high reactivity cathode electrode of OLEDs. Recent development of advanced OLEDs such as top-emitting and flexible OLEDs requires direct encapsulation methods such that the sealing resin is dispensed all over the devices.[4–6] Preparation and characterizations of transparent, UV-curable sealing resins

Y.-Y. Wang, T.-E. Hsieh
Department of Materials Science and Engineering, National Chiao-Tung University, 1001 Ta Hsueh Road, Hsinchu 30050, Taiwan, R. O. C.
E-mail: tehsieh@cc.nctu.edu.tw; vanw31@ms17.hinet.net

Macromol. Chem. Phys. **2007**, *208*, 2396–2402

DOI: 10.1002/macp.200700229

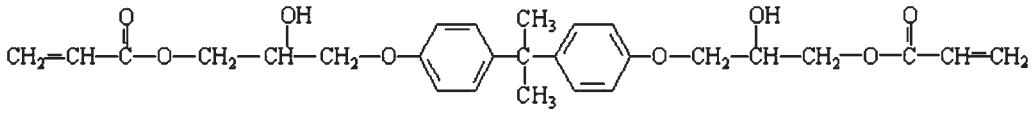

Figure 1. Chemical structure of the oligomer resin serving as the major component in the *co*-polyacrylate/silica nanocomposite resin.

applied to the packaging of advanced OLEDs hence attract a lot of research interests.[7,8]

Satisfactory electrical properties, e.g., low leakage current density, low dielectric constant (ε), and dielectric loss ($\tan\delta$), are crucial to the sealing resins for direct encapsulation in order to enhance the device performance and reduce the power consumption. However, it is well known that the UV curing conditions affect the physical properties of encapsulation resins.[9–11] Inappropriate UV curing deteriorates the mechanical properties[12] and electrical properties[13,14] of polymeric resins. In the previous studies, we reported the preparation and property characterizations of transparent, UV-curable *co*-polyacrylate/silica nanocomposite resins[15] and it has been successfully applied to the direct encapsulation of a bottom-emitting OLED.[16] In this work, a systematic study on the effects of UV curing and post-baking treatments on the electrical properties of such a nanocomposite sealing resins is presented. Experimental results revealed a substantial improvement on the electrical insulation and dielectric properties when silica nanoparticles were formed in *co*-polyacrylate resin matrix via sol-gel process. With appropriate UV curing, the nanocomposite resin film possessing relatively low leakage current density = 1.3 nA $\cdot$ cm^{-2}, $\varepsilon = 3.93$, and $\tan\delta = 0.0472$ could be achieved. However, UV curing with excessive energy density and subsequent post-baking treatment at 80 °C for 1 h were found to degrade the electrical properties of the resin samples. Characterizations of the structural changes and organic/inorganic interfacial interactions were carried out in this work in order to clarify the effects of curing conditions on microstructure and electrical properties of the oligomer resin and nanocomposite resin samples. Degradation mechanisms deduced from the above analyses were also proposed.

Experimental Part

Preparation of the Nanocomposite Resin

The UV-curable *co*-polyacrylate/silica nanocomposite resin was prepared via in situ sol-gel process and its preparation and property characterizations were reported elsewhere.[15] The ingredients of nanocomposite resins were the oligomer (bisphenol A epoxy diacrylate, see Figure 1 for its chemical structure) purchased from Sartomer Co., the radical photopolymerization initiator (1-hydroxycyclohexylphenyl ketone) obtained from Chembridge International Co., acrylic acid and tetraethyl orthosilica (TEOS) purchased from Aldrich Chemicals Co. Preparation of nanocomposite resin is briefly described as follows. First, TEOS and appropriate amount of acrylic acid were sequentially added into a three-necked flask containing oligomer heated at 80 °C. The whole mixture was stirred constantly for 24 h to ignite the in situ sol-gel reaction and the H_2O molecules necessary for hydrolysis reaction were acquired from the moisture in the ambient at about 60% RH. The composition of nanocomposite resin sample is listed in Table 1. After the completion of sol-gel reaction, about 5.0 wt.-% of photoinitiator was added into the above mixture and the stirring was followed to complete the preparation of UV-curable nanocomposite resin samples. A representative microstructure of UV-cured nanocomposite resin obtained by transmission electron microscopy (TEM) is shown in Figure 2.

Property Characterizations

The metal-insulator-metal (MIM) structure was prepared for the electrical property measurements by first coating Al on Si wafer to serve as the bottom electrode. The oligomer and nanocomposite resins were then respectively coated on the Al-coated wafer substrates by using a doctor-blade system. Subsequent photopolymerization of the resins was carried out in a UV oven (CL-1000, UVP) in which the UV irradiation comes from an array of five 8 W dual bipin discharge tubes emitting UV light within the wavelength range of 315–340 nm in air ambient. The UV exposure energy density was set at three different levels, 4.75, 9.5, and 19.0 J $\cdot$ cm^{-2}, in order to investigate the effects of curing energy density on electrical properties of resin samples. The temperature inside the UV oven was below 50 °C during UV curing. After UV curing, parts of the samples were further subjected to a post-baking treatment at 80 °C for 1 h. The top electrode consisting of Ti, Cu, and Au was then deposited on all cured samples to form the MIM structure for subsequent electrical measurements. The breakdown voltage and leaking current density of all samples were evaluated by using an HP 4156B semiconductor parameter

Table 1. Ingredients of nanocomposite sample.

Sample designation	Oligomer/acrylic acid/TEOS[a)]
	mol-%
Nanocomposite	25.15: 31.40: 43.45

[a)] The inorganic content in nanocomposite identified via TGA was about 11.12 wt.-%.[15]

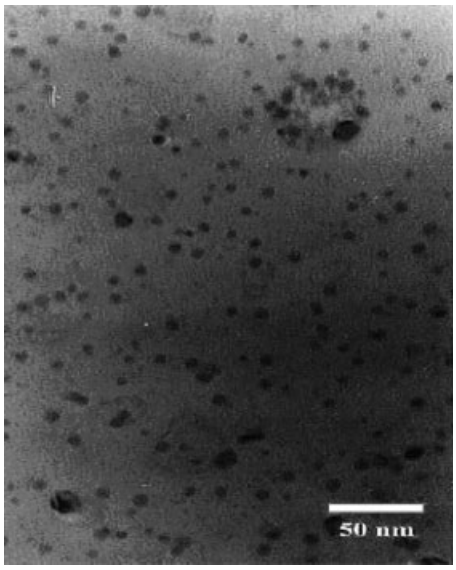

Figure 2. TEM micrograph of the nanocomposite resin prepared in this work.

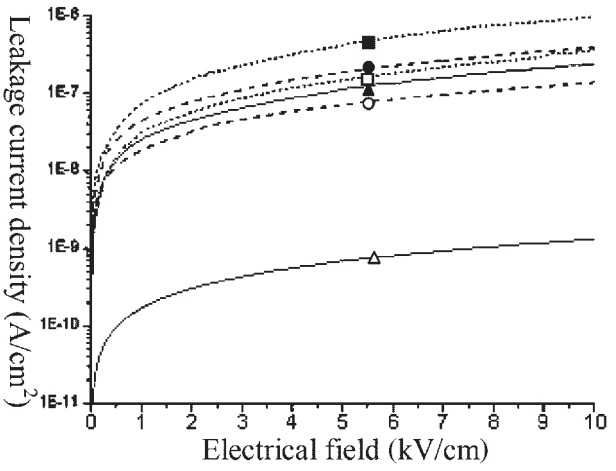

Figure 3. Leakage current density versus electrical field of oligomer cured at 4.75 J · cm^{-2}(—▲—), 9.5 J · cm^{-2}(–●–), 19.0 J · cm^{-2}(··■··) and nanocomposite resins cured at 4.75 J · cm^{-2}(—△—), 9.5 J · cm^{-2}(–○–), 19.0 J · cm^{-2}(··□··), respectively.

analyzer in conjunction with a probe station. The dielectric properties of samples, ε and tanδ, were measured by a C-V system (Keithley, 82-DOS) or an HP 4194A impedance analyzer operating at a frequency of 1 MHz.

The glass transition temperature (T_g) and viscoelastic properties of UV-cured nanocomposite resin were evaluated by a dynamic mechanical analyzer (TA2980, DMA) at a heating rate of 5 °C · min^{-1} and a frequency of 1 Hz. Thermogravimetric analyzer (TA-Q500, TGA) was utilized to identify the 5.0% weight loss temperature ($T_{5\%WL}$) of the oligomer and nanocomposite resins cured at different UV curing energy densities. The TGA data were also transformed to plot the derivative thermogravimetry (DTG) curves. The chemical structures of UV-cured specimens about 60 μm in thickness were analyzed by a Fourier transform infrared spectrometer (Nicolet Protégé 460) in the wave number range of 400–4 000 cm^{-1}. The chemical structures of nanosilica particles in nanocomposite resins were also identified by a Varian UnityInova 500 NMR.

Results and Discussion

Electrical Properties

The leakage current densities of the oligomer and nanocomposite resin films subjected to various UV curing energy densities without post-baking treatment were presented in Figure 3. In the measured voltages ranging from 0 to 100 V, no obvious electrical breakdown was observed in all samples. All resin specimens cured at low UV energy density possess low leakage current densities and, the leakage current density increases with the increase in UV curing energy density. For instance, as shown in Figure 3, at the applied field of 10 kV · cm^{-1} the oligomer and nanocomposite resin films cured at 4.75 J · cm^{-2}, respectively possess low leakage current densities about 235 and 1.3 nA · cm^{-2} while the same resin samples exhibit high leakage current densities about 966 and 371 nA · cm^{-2} after being UV-cured at 19 J · cm^{-2}. Leakage current density measurement indicated that the embedment of nanosilica particles in resin matrix benefited the electrical insulation and hence the nanocomposite film comprised of a much lower leakage current density than that of the oligomer film cured at the same UV curing energy density. Further, the leakage current density increases with the increase in UV curing energy density regardless of the resin sample type.

The lower leakage current density of nanocomposite resins is attributed to the formation of fine-dispersed nanoscale silica particles in the resin matrix. Those intercalated inorganic particles suppress the migration of charge carriers through resin matrix and hence improve the electrical properties. Since high UV irradiation affects the molecular structure of polymeric resins,[17] deterioration of electrical properties of resin samples presented above was attributed to structural changes in the organic portion of samples. Relating characterizations to identify the structural change and degradation mechanism of resin samples are described in the following sections.

Figure 4 presents the effects of post-baking treatment on the electrical insulation of nanocomposite resins; nevertheless, such a thermal treatment deteriorates the electrical properties of samples. For instance, post-baking treatment raises the leakage current density from 1.3 to 45.7 nA · cm^{-2} at the applied field of 10 kV · cm^{-1} for the nanocomposite sample cured at 4.75 J · cm^{-2}.

Macromolecular Journals
DOI: 10.1002/macp.200700229

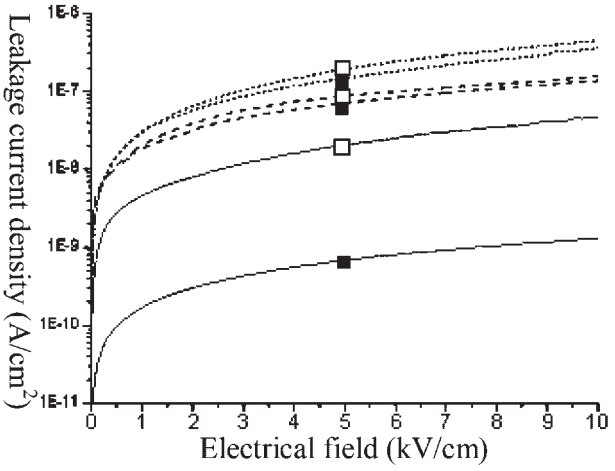

Figure 4. Leakage current density versus electrical field of nanocomposite resins cured at 4.75 J · cm^{-2} (—■—), 4.75 J · cm^{-2} (—□—) with post-baking, 9.5 J · cm^{-2} (– ■ –), 9.5 J · cm^{-2} (– □ –) with post-baking, 19.0 J · cm^{-2} (···■···), and 19.0 J · cm^{-2} (···□···) with post-baking.

Dielectric properties (ε and tanδ) of the oligomer and nanocomposite samples possessing the lowest leakage current densities (i.e., cured at 4.75 J · cm^{-2}) were also measured and the results were presented in Table 2. It can be seen that the nanocomposite sample possesses smaller ε and tan δ in comparison with the oligomer resin. The values of ε and tan δ for nanocomposite sample cured at 4.75 J · cm^{-2} are, respectively 3.93 and 0.0472, which are lower than 8.71 and 0.0713 of the oligomer resin cured at the same UV energy density. This indicates that the formation of nanosized silica particles in the *co*-polyacrylate resin matrix also benefits the dielectric properties. Further, all samples subjected to the post-baking exhibit higher ε and tanδ. Such a thermal treatment hence could not improve the electrical properties of the nanocomposite resins prepared in this work.

Chemical Structure and Thermal Analyses and Their Relationships to Electrical Properties

Figure 5(a) and (b) respectively depict the FTIR spectra of the oligomer and nanocomposite resins cured at different

Table 2. Dielectric properties of resin samples cured at 4.75 J · cm^{-2}.

Resin	Post-baking	ε	tanδ
Oligomer	No	8.71	0.0713
	Yes	9.35	0.0815
Nanocomposite	No	3.93	0.0472
	Yes	5.28	0.0548

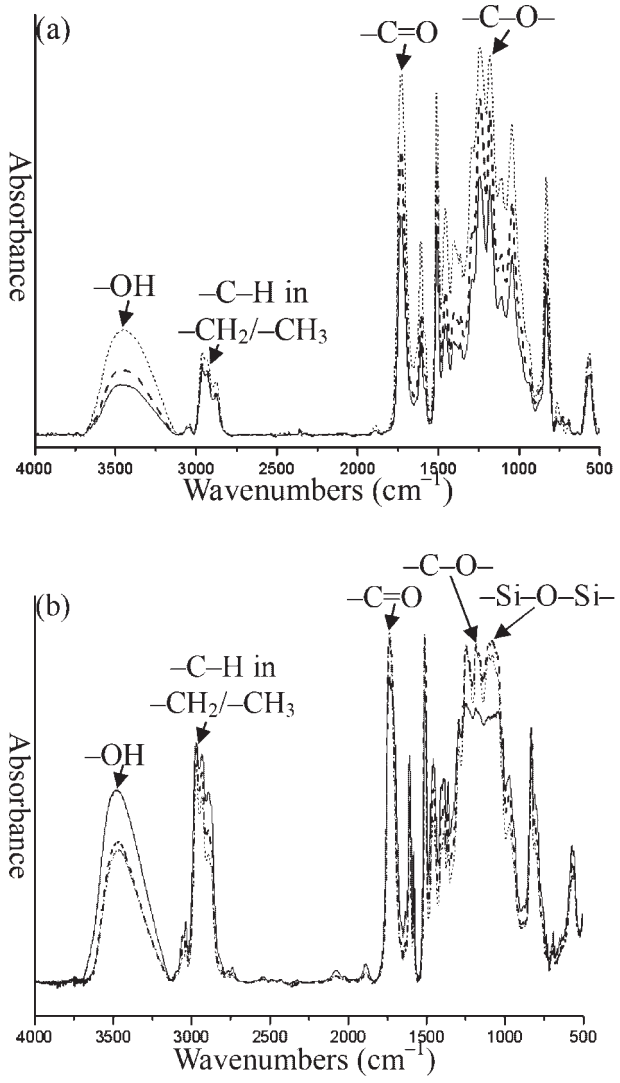

Figure 5. FTIR spectra of (a) the oligomer and (b) the *co*-polyacrylate/silica nanocomposite resins cured at 4.75 (——), 9.5 (– – –), and 19.0 (·····) J · cm^{-2}.

UV energy densities. During FTIR characterization, nitrogen gas was purged into the sample chamber to eliminate the interferences resulting from CO_2, CO, and H_2O in the ambient. As shown in Figure 5(a), continuous rise of functional bands absorbance, for examples, 3 460 cm^{-1} (s, OH), 1 730 cm^{-1} (vs, C=O), and 1 180 cm^{-1} (s, C–O), indicates amplification of oxidized structures in the oligomer chains as a function of the UV curing energy density. In order to preciously identify the occurrence of photooxidation during UV exposure, the relative absorbance ratios of the above functional groups to –C–H in benzene for each of the spectra were calculated and the results are listed in Table 3. The difference of ratios in oligomer samples indicates the occurrence of photooxidation. For example, the ratio of –C=O in UV-cured oligomer chains increases with the curing energy densities, e.g.,

Table 3. Absorbance ratio of designated functional groups in Figure 5.

Functional groups	UV curing energy density for oligomer			UV curing energy density for nanocomposite		
	$J \cdot cm^{-2}$			$J \cdot cm^{-2}$		
	4.75	9.5	19	4.75	9.5	19
–C–O–/–C–H in benzene	3.35	3.61	3.83	2.39	8.17	13.13
–C=O/–C–H in benzene	2.95	3.28	3.64	2.40	7.84	12.55
–O–H/–C–H in benzene	0.67	0.88	1.05	1.49	2.36	3.23
–Si–O–Si–/–C–H in benzene	–	–	–	2.36	8.30	12.58

2.95 for 4.75 $J \cdot cm^{-2}$-cured oligomer and 3.64 for 19 $J \cdot cm^{-2}$-cured oligomer. It is known that the UV irradiation results in crosslinking during the polymerization of the resin; however, excessive UV exposure causes either photooxidation and/or photodegradation of the polymer by inducing the scission of chemical bonds in polymeric chains.[17–19] The FTIR characterization of oligomer resins subjected to high UV curing energy density presented above clearly confirmed the occurrence of photooxidation in the resin matrix.

In accordance with the absorbance ratio increments of –C–O–, –C=O, and –O–H in UV-cured nanocomposite samples listed in Table 3, photooxidation similarly occurred in nanocomposite resins. Further, as indicated by the degradation of thermal stability shown by TGA analysis, photodegradation induced by the scission of short polymer chains also occurs in nanocomposite resins. Table 4 lists the $T_{5\%WL}$ of the oligomer and nanocomposite resins subjected to various UV curing energy densities and Figure 6 presents the DTG analysis of nanocomposite resins. For the oligomer resin, a relatively small $T_{5\%WL}$ decrease indicates that the UV curing energy density has very little influence on its thermal stability. Nevertheless, significant deterioration of thermal stability was observed in the nanocomposite specimens subjected to UV curing at high energy density, e.g., the $T_{5\%WL}$ decreased from 175.9 to 161.7 °C when UV curing energy density was raised from 4.75 to 19 $J \cdot cm^{-2}$. Owing to the existence of newly formed small molecules such as ethyl acrylate or acrylic anhydride in nanocomposite resin,[15] the DTG curves of nanocomposite resin consist of one major peak at about 430 · C and one broad peak at around 190 · C as shown in Figure 6(a). The continuous decline in derivative weight of the major

Table 4. $T_{5\%WL}$ of oligomer and nanocomposite resins obtained by TGA.

Curing condition	Oligomer	Nanocomposite
$J \cdot cm^{-2}$	°C	°C
UV-cured at 4.75	232.2	175.9
UV-cured at 9.5	231.5	169.1
UV-cured at 19	229.9	161.7

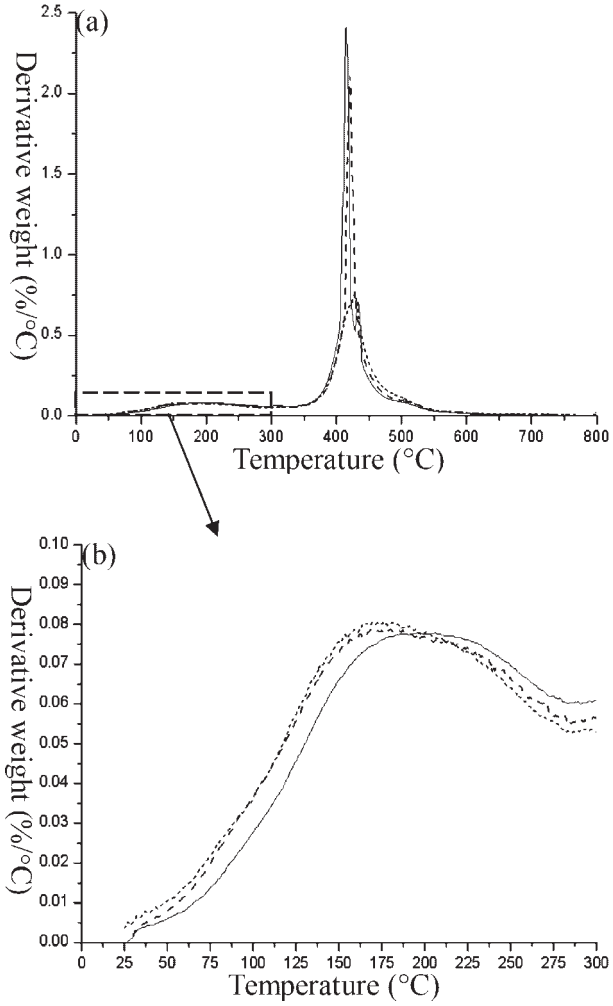

Figure 6. DTG results of (a) the *co*-polyacrylate/silica nanocomposite resins cured at 4.75 (——), 9.5 (– – –), and 19.0 (·····) $J \cdot cm^{-2}$ and (b) enlargement of portion in (a).

Macromolecular Journals
DOI: 10.1002/macp.200700229

peak indicated that the short side chains in the UV-crosslinked *co*-polyacrylate structure degrades into radical/ionic polymeric segments by the breakage of chemical bonds during UV exposure.[15,17] A noticeable feature in Figure 5 and Table 3 is the emergence of 1 090 cm^{-1} (s, Si–O–Si) for the nanocomposite resins when UV curing energy density becomes high. It can also be seen that the absorbance ratio of this peak increases with the increase in UV curing energy density. This likely resulted from the sol–gel reaction of $-O-CH_2CH_3$ and –OH groups capped on nanosilica particles, as revealed by NMR characterization shown in Figure 7.[20] Consequently, excessive UV curing induced the photooxidation and generated the radical/ionic segments in organic matrix and –Si–O–Si– structure in the vicinity of silica particles. Finally, we note that the post-baking treatment barely affects the chemical structures of resin samples in accordance with the highly similar spectra obtained prior to and posterior to the thermal treatment.

It is known that polar groups in polymers may absorb moisture molecules in ambient and establish permeation paths in the organic portion. As revealed by the above chemical structure analyses, excessive UV exposure induced more polar groups and hence more moisture molecules trapped in the resin matrix. When an external bias was applied, the charge carriers might migrate along these newly established permeation paths and thereby raised the leakage current in the resin samples subjected to excessive UV curing. Furthermore, photodegradation generated radical/ionic segments in the nanocomposite resins. This builds up additional permeation paths in the samples and exasperates the charge carrier migration in the excessively cured nanocomposite resin samples. A dramatic increase in the leakage current density was hence observed in the nanocomposite sample cured by 19 $J \cdot cm^{-2}$.

The purposes of post-baking treatment are to terminate the photoreaction process and enhance the structure rigidity of polymeric resins. It seems such a thermal treatment should improve the electrical properties; however, the data presented in the previous section show an opposite result. It was speculated that the post-baking treatment carried out in this work may bring the oxidized groups and radical/ionic segments resulted from excessive UV curing much closer to each other. This increase in the molecule packing reduces the hopping distance of charge migration, which, in turn, results in an increase in the leakage current in nanocomposite resins subjected to post-baking treatment.

Relationship between Electrical Properties and Inorganic Particles/Polymeric Chains Interaction via Dynamic Mechanical Analysis

Dissipation factor obtained via DMA is very sensitive to the structure transformation of polymers, the intensity profile and peak position of the dissipation factor are commonly adopted to explore the behaviors of polymeric chains. In order to investigate the interactions between inorganic particles and polymeric chains in nanocomposite resin samples, we prepared the resin samples cured at a unique energy density of 6 $J \cdot cm^{-2}$ for DMA study. Figure 8 presents the dissipation factors obtained by DMA for oligomer and nanocomposite resin samples. It reveals that the T_g of the nanocomposite resin is higher than that of the oligomer resin by about 20 °C and the nanocomposite resin possesses a smaller dissipation factor. The improvements in the above mentioned physical properties resulted from the intercalation of silica nanoparticles embedded in *co*-polyacrylate resin. Furthermore, according to the study on PMMA-SiO_2 nanocomposite,[21] cladding of

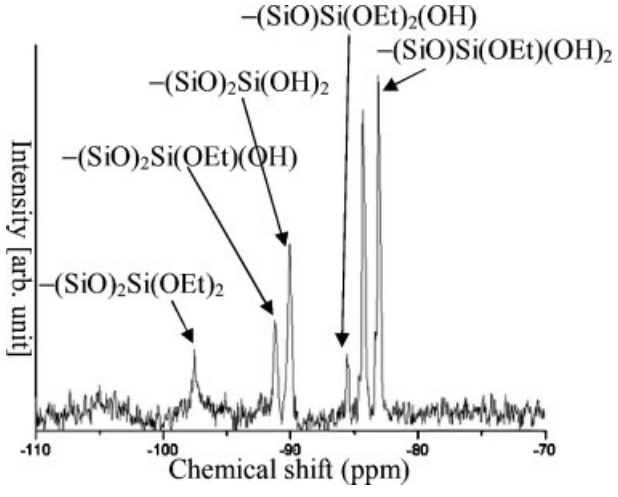

Figure 7. ^{29}Si NMR spectra of this nanocomposite resin.

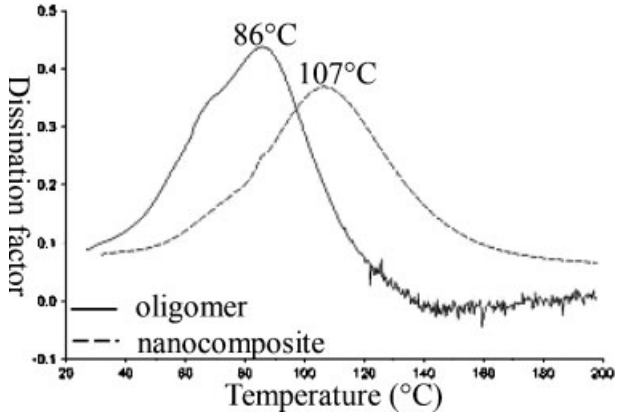

Figure 8. Dissipation factors obtained via DMA for oligomer and co-polyacrylate/silica nanocomposite resin UV-cured at 6 $J \cdot cm^{-2}$. The temperatures specified in the plot are the T_g's of samples.

organic portion on nanosized particles is able to restrict the mobility of polymer chains since the polymer chains were tethered to the organic portion. Analyses presented in the previous section clearly illustrated the capping of $-O-CH_2CH_3$, –OH, and –Si–O–Si– groups on silica nanoparticles. Similarly, the frictions between these organic/inorganic functional groups and polymer chains might restrict the mobility of the *co*-polyacrylate chains and provide a certain contribution to the improvements on T_g and dissipation factor of nanocomposite resins. In addition, the frictions between organic and inorganic portions should be able to inhibit the movements of polar groups in *co*-polyacrylate chains so as to suppress the polarization in nanocomposite resins when external bias was applied. The less the polarization, the less the total electric energy consumed by the dipole motions in nanocomposite resins. Consequently, relatively low values of ε and $\tan\delta$ were observed in nanocomposite resin in comparison with oligomer resin.

Conclusion

In this work, the electrical properties of transparent, UV-curable *co*-polyacrylate/silica nanocomposite resins prepared by in situ sol-gel process were investigated. Experimental results revealed that the embedment of nanoscale silica particles in organic matrix effectively improves the electrical properties of resin samples. The intercalation of inorganic particles effectively inhibited the migration of charge carriers thus reducing the leakage current density of nanocomposite resin samples. Furthermore, the frictions were generated between the organic/inorganic function groups such as $-O-CH_2CH_3$, –OH, and –Si–O–Si– groups capping on silica nano-particles and the *co*-polyacrylate chains. This restricted the chain mobility and improved the dielectric properties of nanocomposite resin samples. With appropriate UV curing process, the nanocomposite resin with satisfactory electrical properties (leakage current density $= 1.3\ \text{nA}\cdot\text{cm}^{-2}$; $\varepsilon = 3.93$; $\tan\delta = 0.0472$) were achieved in this work.

Experimental analyses also found that excessive UV curing results in photooxidation and/or photodegradation in the resin samples. This implied the formation of polar groups and ionic/radical segments in organic matrix and the –Si–O–Si– structure in the vicinity of silica nanoparticles. These organic/inorganic functional groups established additional permeation paths for charge carrier migration and raised the leakage current in the samples. Electrical properties of resin samples hence deteriorated. Though post-baking treatment may terminate the photoreaction process and provide a more rigid structure for resin samples, it brought the polar functional groups in the polymeric chains closer to each other and promoted the current leakage. The post-baking treatment at 80 °C for 1 h carried out in this work hence did not benefit the electrical properties of nanocomposite resin samples.

Acknowledgements: This work was supported by the *Ministry of Education of the Republic of China* with the *Academic Center of Excellence in "Semiconducting Polymers and Organic Molecules for Electroluminance"* under contract no. 91-E-FA04-2-4.

Received: April 24, 2007; Revised: July 22, 2007; Accepted: July 25, 2007; DOI: 10.1002/macp.200700229

Keywords: dielectric properties; microstructure; nanocomposites; photopolymerization

[1] M. T. Gales, C. Gimkiewicz, S. Obi, M. Schnieper, J. Söchtig, H. Thiele, S. Westenhöfer, *Opt. Lasers Eng.* **2005**, *43*, 373.
[2] K. K. Baikerikar, A. B. Scranton, *Polymer* **2001**, *42*, 431.
[3] C. W. Tan, Y. C. Chen, H. P. Chan, N. W. Leung, C. K. So, *Microelectron. Reliab.* **2004**, *44*, 823.
[4] G. H. Kim, J. Oh, Y. S. Yang, L. M. Do, K. S. Suh, *Thin Solid Films* **2004**, *467*, 1.
[5] G. H. Kim, J. Oh, Y. S. Yang, L. M. Do, K. S. Suh, *Polymer* **2004**, *45*, 1879.
[6] K. M. Kim, B. J. Jang, W. S. Cho, S. H. Ju, *Curr. Appl. Phys.* **2005**, *5*, 64.
[7] R. Okuda, K. Miyoshi, N. Arai, M. Tomikawa, G. Ohbayashi, *J. Photopolym. Sci. Technol.* **2002**, *15*, 205.
[8] R. Okuda, K. Miyoshi, N. Arai, M. Tomikawa, *J. Photopolym. Sci. Technol.* **2004**, *17*, 207.
[9] A. A. Basfar, *Polym. Degard. Stab.* **2002**, *77*, 221.
[10] A. A. Basfar, *Polym. Degard. Stab.* **2003**, *82*, 333.
[11] K. Bittner-Rohrhofer, K. Humer, H. Fillunger, R. K. Maix, H. W. Weber, P. E. Fabian, N. A. Munshi, *J. Nucl. Mater.* **2004**, *329*, 1083.
[12] Ch. Chevalier, V. Coste, A. Fontaine, M. Tavlet, *Nucl. Instrum. Methods Phys. Res. B* **1999**, *151*, 438.
[13] K. Shinyama, M. Baba, S. Fujita, *Proc. Int. Symp. Electr. Insul. Mater.* **1998**, p. 387.
[14] M. Ehsani, H. Borsi, E. Gockenbach, J. Morshedian, G. R. Bakhshandeh, A. A. Shayegani, *Proc. Int. Conf. Symp. Solid Dielectr.* **2004**, p. 312.
[15] Y. C. Chou, Y. Y. Wang, T.-E. Hsieh, *J. Appl. Polym. Sci.* **2007**, *105*, 2073.
[16] Y. Y. Wang, T.-E. Hsieh, I. C. Chen, C. H. Chen, *IEEE Adv. Pack.* **2007**, *30*, 421.
[17] D. J. Carlsson, S. Chmela, *"Mechanisms of Polymer Degradation and Stabilisation"*, Elsevier Science, New York 1990.
[18] O. Chiantore, L. Trossarelli, M. Lazzari, *Polymer* **2000**, *41*, 1657.
[19] C. Decker, K. Zahouily, *Polym. Degard. Stab.* **1999**, *64*, 293.
[20] T. Caykara, O. Güven, *Polym. Degard. Stab.* **1999**, *65*, 225.
[21] Y. H. Hu, C. Y. Chen, C. C. Wang, *Polym. Degard. Stab.* **2004**, *84*, 545.

DOI: 10.1002/macp.200700229